

Advances in surface electromyographic signal simulation with analytical and numerical descriptions of the volume conductor

*Original*

Advances in surface electromyographic signal simulation with analytical and numerical descriptions of the volume conductor / Farina, D; Mesin, Luca; Martina, S.. - In: MEDICAL & BIOLOGICAL ENGINEERING & COMPUTING. - ISSN 0140-0118. - STAMPA. - 42:4(2004), pp. 467-476. [10.1007/BF02350987]

*Availability:*

This version is available at: 11583/1913045 since: 2021-06-16T11:34:30Z

*Publisher:*

Springer

*Published*

DOI:10.1007/BF02350987

*Terms of use:*

openAccess

This article is made available under terms and conditions as specified in the corresponding bibliographic description in the repository

*Publisher copyright*

Springer postprint/Author's Accepted Manuscript

This version of the article has been accepted for publication, after peer review (when applicable) and is subject to Springer Nature's AM terms of use, but is not the Version of Record and does not reflect post-acceptance improvements, or any corrections. The Version of Record is available online at: <http://dx.doi.org/10.1007/BF02350987>

(Article begins on next page)

**ADVANCES IN SURFACE ELECTROMYOGRAPHIC SIGNAL  
SIMULATION WITH ANALYTICAL AND NUMERICAL DESCRIPTIONS  
OF THE VOLUME CONDUCTOR**

**Dario Farina, Luca Mesin, Simone Martina**

*Centro di Bioingegneria, Dip. di Elettronica, Politecnico di Torino, Torino, Italy*

**Keywords:** surface EMG, modelling, volume conductor, conductivity tensor

**Running title:** Surface EMG signal simulation

**Correspondence to:**

Dario Farina, PhD

Dipartimento di Elettronica, Politecnico di Torino; Corso Duca degli Abruzzi 24, Torino, 10129 ITALY

Tel. 0039-011-4330476; Fax. 0039-0114330404; e-mail: [dario.farina@polito.it](mailto:dario.farina@polito.it)

**Acknowledgements**

The authors are grateful to prof. Merletti of the Dept. of Electronics of Politecnico di Torino for the useful suggestions provided on this work. This work was supported by the European Shared Cost Project *Neuromuscular assessment in the Elderly Worker* (NEW) (Contract n° QLRT-2000-00139).

## **Authors' biography**

**Dario Farina** graduated *summa cum laude* in Electronics Engineering from Politecnico di Torino, Torino, Italy, in February 1998. During 1998 he was a Fellow of the Laboratory for Neuromuscular System Engineering in Torino. In 2001 he obtained the PhD degree in Electronics Engineering at Politecnico di Torino and at the Ecole Centrale de Nantes, Nantes, France. Since 2002 he is Research Assistant Professor at the same University. His main research interests are in the areas of signal processing applied to biomedical signals, modeling of biological systems, and basic and applied physiology of the neuromuscular system. Dr. Farina is a Registered Professional Engineer.

**Luca Mesin** graduated in Electronics Engineering in December 1999 from Politecnico di Torino, Torino, Italy, and received the PhD degree in Applied Mathematics in 2003 from the same University. Since March 2003, he is a Fellow of the Laboratory for Neuromuscular System Engineering in Torino. His main research interests concern signal processing of biomedical signals and modeling of biological systems.

**Simone Martina** was born in 1978. He is a PhD candidate at the Dept. of Mechanical Engineering of Politecnico di Torino, Torino, Italy, and, since 2003, a Fellow of the Laboratory for Neuromuscular System Engineering, Politecnico di Torino. His research interests are in EMG signal processing and modelling.

## **ABSTRACT**

Surface electromyographic (EMG) signal modeling is important for signal interpretation, testing of processing algorithms, detection system design, and didactic purposes. Various surface EMG signal models have been proposed in the literature. In this study we focus on 1) the proposal of a method for modeling surface EMG signals by either analytical or numerical descriptions of the volume conductor for space-invariant systems, and 2) the development of advanced models of the volume conductor by numerical approaches, accurately describing not only the volume conductor geometry, as mainly done in the past, but also the conductivity tensor of the muscle tissue. For volume conductors that are space-invariant in the direction of source propagation, the surface potentials generated by any source can be computed by one-dimensional convolutions, once the volume conductor transfer function is derived (analytically or numerically). Conversely, more complex volume conductors require a complete numerical approach. In a numerical approach, the conductivity tensor of the muscle tissue should be matched with the fiber orientation. In some cases (e.g., multi-pinnate muscles) accurate description of the conductivity tensor may be very complex. A method for relating the conductivity tensor of the muscle tissue, to be used in a numerical approach, to the curve describing the muscle fibers is presented and applied to representatively investigate a bi-pinnate muscle with rectilinear and curvilinear fibers. The study thus propose an approach for surface EMG signal simulation in space invariant systems as well as new models of the volume conductor using numerical methods.

## 1. INTRODUCTION

The simulation of surface EMG signals is important for the estimation of physiological variables (inverse problem) (VAN OOSTEROM, 1998), a deeper understanding of the physiological mechanisms (KLEINE *et al.*, 2001), a proper choice of the detection system parameters (DIMITROV *et al.*, 2003; FARINA *et al.*, 2004a), the interpretation of experimental results (DIMITROVA and DIMITROV, 2003; ROELEVELD *et al.*, 1997), and didactic purposes (MERLETTI *et al.*, 1999a; MERLETTI *et al.*, 1999b; STEGEMAN *et al.*, 2000). The main steps in the development of an EMG model are 1) the description of the source, i.e., the modeling of the generation, propagation, and extinction of the intracellular action potential, 2) the mathematical description of the local properties of the volume conductor (with a formulation based on partial differential equations), 3) the analysis of the geometry of the volume conductor and of the boundary conditions, and 4) the modelization of the detection system, i.e., of the spatial filter applied to the skin potential distribution (spatial arrangement, shape and size of the electrodes, inter-electrode distance). Different approaches have been proposed for the description of the source, including generation, traveling, and extinction phenomena (DIMITROV and DIMITROVA, 1998; DIMITROVA, 1974; DIMITROVA *et al.*, 2001; GOOTZEN *et al.*, 1991; GRIEP *et al.*, 1982; GYDIKOV *et al.*, 1986; KLEINPENNING *et al.*, 1990; MCGILL and HUYNH, 1988; PLONSEY, 1977). The second and third issues are related to the description of the tissues separating the sources from the detecting electrodes. In this work we will mainly focus on these two topics. For the description of the source we will adapt a previously proposed approach (FARINA & MERLETTI, 2001a), while for the analysis of the detection system we refer to previous work (DIMITROVA *et al.*, 1999a; 1999b; 2001; FARINA & MERLETTI, 2001a; 2001b; HELAL & BOUISSOU, 1992; REUCHER *et al.*, 1987a; 1987b).

The volume conductor can be described either analytically (BLOK *et al.*, 2002; DIMITROV and DIMITROVA, 1998; FARINA *et al.*, 2003a; GOOTZEN, 1990; GOOTZEN *et al.*, 1991) or numerically (LOWERY *et al.*, 2002; SCHNEIDER *et al.*, 1991). Analytical solutions can be obtained only in specific cases, while numerical methods are necessary when considering more complex conditions.

Nevertheless, analytical solutions are valuable for many reasons: 1) to determine the theoretical dependence of the solution on specific parameters of the system, 2) to check the accuracy of numerical methods, and 3) to reduce the computational time (e.g., when modeling is used for solving the inverse problem). For these reasons, it is important to focus on analytical solutions when this is feasible and to apply numerical methods only when the geometry of the volume conductor and the properties of its conductivity tensor are too complex. Moreover, the use of complex and time consuming numerical methods should be justified by applications which indeed require the increased complexity with respect to an analytical solution (which is relatively fast and exact). Thus, it is of primary relevance to foresee how a more detailed description of the volume conductor may have an impact on the specific research questions at hand (STEGEMAN *et al.*, 2000).

In the last years, efforts have been devoted to the simulation of surface EMG signals generated in complex volume conductors (BLOK *et al.*, 2002; FARINA *et al.*, 2003a; LOWERY *et al.*, 2002; MESIN and FARINA, 2004). In this study we present the solution of the problem for a number of geometries, underlining recent advances in the analytical solutions and presenting new insights into the numerical approach. In particular, we will focus on the necessity of carefully describing the conductivity tensor of the volume conductor in a numerical approach rather than focusing exclusively on the accurate description of the geometry, as mostly done in the past. Moreover, to decrease the computational time, we will present the possibility of using, in the same model, numerical methods for the description of the volume conductor and analytical methods for the modelization of the source. Representative examples of advanced simulations of surface EMG signals (e.g., with bi-pinnate muscles or in the presence of tissue in-homogeneities) will be presented.

## **2. METHODS**

### **2.1. Description of the source**

The modeling of the generation, propagation, and extinction of the intra-cellular action potential has been performed in the past following different approaches (DIMITROV and DIMITROVA, 1998; DIMITROVA, 1974; GOOTZEN *et al.*, 1991; GRIEP *et al.*, 1982; MCGILL and HUYNH, 1988). The general assumption is that the integral of the current density over the muscle fiber length is zero in each instant of time. Following this assumption, FARINA and MERLETTI (2001a) proposed a mathematical description of the generation, propagation, and extinction of the intra-cellular action potential along the fiber as a function of space and time. The description can be adapted to propagation of the intra-cellular action potential along any path, as follows (multiplicative constants are not reported):

$$i(s,t) = \frac{d}{ds} \left[ \psi(\gamma(s - s_i - vt)) p_{L_1}(\gamma(s - s_i - L_1/2)) - \psi(\gamma(-s + s_i - vt)) p_{L_2}(\gamma(s - s_i + L_2/2)) \right] \quad (1)$$

where  $\gamma$  is the path of propagation,  $s$  is the curvilinear abscissa defined along  $\gamma$ ,  $t$  is the time coordinate;  $i(s,t)$  is the current density source;  $v$  the propagation velocity of the source;  $\psi(\gamma(s))$  the first derivative of  $V_m(\gamma(-s))$  (with  $V_m(\gamma(s))$  the intracellular action potential);  $p_L(\gamma(s))$  a function that takes value 1 for  $-L/2 \leq s \leq L/2$  and 0 otherwise;  $\gamma(s_i)$  the position of the end-plate;  $L_1$  and  $L_2$  the semi-lengths of the fiber from the end-plate to the right and to the left tendon, respectively.

Eq. (1) is the generalization of the concepts presented by FARINA and MERLETTI (2001a) for a path of propagation which may be defined by any curve. Eq. (1) implies the generation of two intra-cellular action potentials at the end-plate, their propagation along two semi-fibers of different length, and their extinction at the tendon endings. The assumption of the line source model (DIMITROVA, 1974; GRIEP *et al.*, 1982; JOHANNSEN, 1986; PLONSEY, 1977) in Eq. (1) implies that the current density source is proportional to the second derivative of the intra-cellular action potential. Note that for simulating the muscle tissue it should be assumed that the direction of propagation of the source corresponds to the direction of highest conductivity while the transverse directions are those of lowest conductivity. Thus, the description of the source in Eq. (1) also implies a description of the conductivity tensor in each point of the muscle fiber.

## 2.2 Description of the volume conductor

The local electrical behavior of the volume conductor is described by the Poisson's equation (PLONSEY, 1977):

$$\nabla \cdot (\underline{\underline{\sigma}} \nabla \varphi) = -I \quad (2)$$

where  $\varphi$  is the potential (V),  $I$  is the current density source (A/m<sup>3</sup>), and  $\underline{\underline{\sigma}}$  the conductivity tensor (S/m).

Poisson's equation is the mathematical model of the volume conductor. To obtain a mathematical problem, whose solution provides the electric potential at each point of the volume conductor, the local properties of the volume conductor should be considered together with the specification of the geometry of the system and of the conditions to be imposed on its boundaries. These conditions are usually Neumann homogeneous conditions (EVANS, 1998):

$$\frac{\partial \varphi}{\partial n} = 0 \quad \partial \Omega, \quad (3)$$

where  $n$  is the versor normal to the boundary  $\partial \Omega$ , as the volume conductor is assumed insulated.

Some simple models of volume conductors of practical interest have been considered in the literature, and analytical solutions are available for them. The simplest model is that of a homogeneous, isotropic, infinite medium, for which the conductivity tensor is constant in space and time (CLARK and PLONSEY, 1968; DIMITROV and DIMITROVA, 1998). Rectilinear or curvilinear fibers inclined with respect to the detection surface have been simulated in homogeneous volume conductors but without adapting the conductivity properties to fiber direction (DIMITROV & DIMITROVA, 1980; DIMITROVA *et al.*, 1999a; XIAO *et al.*, 1995). More realistic models are comprised of planar (FARINA and MERLETTI, 2001a) (conductivity tensor  $\underline{\underline{\sigma}} = \sigma_{xx} \vec{i}\vec{i} + \sigma_{yy} \vec{j}\vec{j} + \sigma_{zz} \vec{k}\vec{k}$ ) (Figure 1a) or cylindrical (BLOK *et al.*, 2002; FARINA *et al.*, 2003a; GOOTZEN, 1990) (conductivity tensor  $\underline{\underline{\sigma}} = \sigma_{\rho\rho} \vec{\rho}\vec{\rho} + \sigma_{\theta\theta} \vec{\theta}\vec{\theta} + \sigma_{zz} \vec{k}\vec{k} = \underline{\underline{\sigma}}(\rho)$ ) layers (Figure 1d,f).



## Figure 1 about here

More complex systems are the models of bi-pinnate muscles (MESIN & FARINA, 2004) or of a muscle with fibers inclined with respect to the detection surface which include an adaptation of conductivity tensor to the fiber direction (Figure 1b,c,g,h) (MESIN & FARINA, 2004).

The choice of the mathematical tool for solving the forward problem depends on the local properties (i.e., on the conductivity tensor) and on the geometry of the volume conductor.

### 2.2.1 Conductivity tensor

Most EMG models consider a quasi static condition, for which the local electrical properties of the volume conductor are fully determined by its conductivity tensor. In general a volume conductor may present a conductivity tensor which is function of position, time, and potential. If the conductivity tensor is a function of the local potential, the volume conductor is non-linear, and Poisson's equation is a non-linear equation. Fairly simpler problems concern linear volume conductors. In such cases, the conductivity of the volume conductor does not depend on the potential. Transformation methods can be used to solve Poisson's problem in the case of linear volume conductors. The transform will depend on the geometry. Simpler Poisson's problems are those concerning autonomous systems. In such cases, the conductivity tensor is only a function of position, constant in time. In this study we will focus on linear, autonomous systems.

Two further concepts which are useful to classify and study volume conductors are isotropy and homogeneity. Isotropy is defined by the following condition (ERINGEN, 1967; 1971):

$$\underline{\underline{\sigma}} R\vec{V} = R\underline{\underline{\sigma}}\vec{V}, \quad (4)$$

where  $\underline{\underline{R}}$  indicates an arbitrary rotation matrix, and  $\vec{V}$  is an arbitrary vector. An isotropic volume conductor presents the same conductivity in all directions.

As isotropy implies invariance under rotations, homogeneity imposes invariance under translations. Thus, a homogeneous volume conductor has a conductivity tensor constant in each point. Homogeneity can also be defined in specific directions. For example, in a Cartesian coordinate system, a volume conductor homogeneous in the  $z$  direction is characterized by the following conductivity tensor:

$$\underline{\underline{\sigma}}(x, y, z) = \underline{\underline{\sigma}}(x, y) \quad (5)$$

Homogeneity is an important feature of a volume conductor when the direction of propagation of the source coincides with a homogeneity direction, as will be detailed below.

Modeling of the conductivity tensor of the muscle tissue has been neglected in the literature on EMG simulation, as Cartesian or cylindrical conductivity tensors have been studied, even in the case of sources traveling along a general curvilinear path (DIMITROVA *et al.*, 1999a; MERLETTI *et al.*, 1999; XIAO *et al.*, 1995). Since the conductivity of the muscle tissue depends on the direction of the muscle fibers, the conductivity tensor of this tissue should depend point-by-point on the fiber orientation.

Let's consider an arbitrary muscle tissue, whose conductivity tensor can be expressed as:

$$\underline{\underline{\sigma}} = \sigma_l \hat{v}_l \hat{v}_l + \sigma_t \hat{v}_m \hat{v}_m + \sigma_t \hat{v}_{tb} \hat{v}_{tb} \quad (6)$$

where the subscript  $l$  stands for longitudinal and  $t$  for transversal coordinates with respect to the fiber direction, and  $\hat{v}_l, \hat{v}_m, \hat{v}_{tb}$  are the longitudinal, normal, and binormal vectors relative to the fiber path, respectively. In general, such vectors are functions of position. They can be computed from the analytical expression of the path of propagation. Without lack of generality, we will assume that the longitudinal and transverse conductivities,  $\sigma_l$  and  $\sigma_t$  [Eq. (6)], are constant. This means that, given the direction of the muscle fiber in a specific point, the conductivity of the tissue longitudinal and transversal to this direction are constant (in each point these two directions change if the fiber is curvilinear). Furthermore, the transverse conductivities will be assumed equal for the normal and binormal directions. A generalization of the previous constraints is straightforward.

Poisson's equation in a Cartesian system for the general conductivity tensor introduced above can be obtained by introducing the Cartesian representation of the curvilinear differential operators (gradient and divergence) as follows:

$$\nabla \cdot (\underline{\underline{\sigma}} \nabla(\bullet)) = \begin{pmatrix} \partial_x & \partial_y & \partial_z \end{pmatrix} \left[ (\sigma_l \vec{v}_l \vec{v}_l + \sigma_t \vec{v}_m \vec{v}_m + \sigma_t \vec{v}_{tb} \vec{v}_{tb}) \begin{pmatrix} \partial_x \\ \partial_y \\ \partial_z \end{pmatrix} \right] \quad (7)$$

where  $\partial_x$ ,  $\partial_y$ , and  $\partial_z$  indicate the partial derivative operators in Cartesian coordinates and  $\vec{v}_l, \vec{v}_m, \vec{v}_{tb}$  are the versors corresponding to  $\hat{v}_l, \hat{v}_m, \hat{v}_{tb}$ . Eq. (7) can be used in general to determine the conductivity tensor given the propagation path of the source.

As an example, let's consider a muscle tissue with rectilinear bipinnate fibers (MESIN and FARINA, 2004). The conductivity tensor is in this case:

$$\underline{\underline{\sigma}} = \begin{bmatrix} \sigma_l \sin^2(\omega) + \sigma_t \cos^2(\omega) & 0 & (\sigma_t - \sigma_l) \cos(\omega) \sin|\omega| \\ 0 & \sigma_t & 0 \\ (\sigma_t - \sigma_l) \cos(\omega) \sin|\omega| & 0 & \sigma_l \cos^2(\omega) + \sigma_t \sin^2(\omega) \end{bmatrix} \quad (8)$$

where  $\omega$  is the pinnation angle (i.e., the angle between the  $z$  axis and the fibers, placed in planes of constant  $y$  coordinate). In Eq. (8) the angles on the two sides of the pinnation plane  $x = 0$  are assumed equal except for the sign.

Similarly we may consider a muscle tissue with fibers following a non-rectilinear direction of propagation and with two orientations (bi-pinnate muscle). Let's assume that the fibers are in a semi-cylindrical muscle tissue, distributed along a path described by the following helicoidal curve (Figure 2):

$$\gamma(\lambda) = \begin{pmatrix} r \cos(\lambda) \\ r \sin(\lambda) - \beta \\ \alpha \lambda - \delta \end{pmatrix} \quad (9)$$

where  $r$  is the radius of the cylinder,  $\alpha$  is a parameter related to the pinnation angle, and  $\beta$  and  $\delta$  are constants identifying a specific fiber. The longitudinal, normal, and binormal versors are in this case:

$$\begin{aligned}\vec{v}_l &= \begin{pmatrix} -r \sin(\lambda) \\ r \cos(\lambda) \\ \alpha \end{pmatrix} = \begin{pmatrix} -\sqrt{r^2 - x^2} \\ x \\ \alpha \end{pmatrix}; & \vec{v}_m &= \begin{pmatrix} -r \cos(\lambda) \\ -r \sin(\lambda) \\ 0 \end{pmatrix} = \begin{pmatrix} -x \\ -\sqrt{r^2 - x^2} \\ 0 \end{pmatrix}; \\ \vec{v}_{tb} &= \begin{pmatrix} \alpha r \sin(i) \\ -\alpha r \cos(t) \\ r^2 \end{pmatrix} = \begin{pmatrix} \alpha \sqrt{r^2 - x^2} \\ -\alpha x \\ r^2 \end{pmatrix}\end{aligned}\quad (10)$$

The pinnation angle is obtained from the expression of  $\vec{v}_l$ :

$$\theta = \frac{1}{2} \arccos\left(\frac{\alpha^2 - r^2}{\alpha^2 + r^2}\right) \quad (11)$$

The source in Eq. (1) can be described substituting the expression of  $\gamma(\lambda)$  at hand, selecting one fiber (i.e., choosing  $\beta = \beta_0$ ,  $\delta = \delta_0$ ), and evaluating the curvilinear abscissa.

Using the normalized versions of the vectors for the general expression (7), algebraic calculations (rather long but straightforward) yield the following expression of the conductivity tensor in a Cartesian system:

$$\underline{\underline{\sigma}} = \frac{1}{\alpha^2 + r^2} \begin{bmatrix} (r^2 - x^2)\sigma_l + (\alpha^2 + x^2)\sigma_t & x\sqrt{r^2 - x^2}(\sigma_t - \sigma_l) & \alpha\sqrt{r^2 - x^2}(\sigma_t - \sigma_l) \\ x\sqrt{r^2 - x^2}(\sigma_t - \sigma_l) & x^2\sigma_l + (r^2 + \alpha^2 - x^2)\sigma_t & \alpha x(\sigma_t - \sigma_l) \\ \alpha\sqrt{r^2 - x^2}(\sigma_t - \sigma_l) & \alpha x(\sigma_t - \sigma_l) & \alpha^2\sigma_l + r^2\sigma_t \end{bmatrix} \quad (12)$$

Using the expression in Eq. (12) with a finite element approach for the description of the volume conductor allows the determination of the potential distribution over the skin surface generated by a current source in the volume conductor of Figure 2 (see Results). Note that the description of the source is strictly linked to the determination of the conductivity tensor.

Eq. (7) provides a general way to compute the conductivity tensor given the direction of the muscle fibers. The bipinnate muscles with rectilinear or curvilinear fibers described above are only examples of the application of the method. In general, given the parametric representation of the curve defining the muscle fibers [as in Eq. (9)], it is possible to compute the corresponding longitudinal, normal, and binormal versors [as done, for the example of the curvilinear bipinnate

muscle, in Eq. (10)]. From the longitudinal, normal, and binormal vectors, Eq. (7) allows the determination of the conductivity tensor [here given by Eqs. (8) and (12)].

**Figure 2 about here**

### 2.2.2 Geometry

To address the forward problem analytically, a simplified model of volume conductor has to be studied. For convenience, the volume conductor is usually assumed infinite, at least in specific directions. This assumption does not significantly affect the solution if the potential decays fast in space relatively to the volume conductor dimensions, so that edge effects are negligible. Such an assumption allows to study the impulsive response (the general solution is then obtained integrating the impulsive response weighted by the actual source). For insulated bounded domains, the derivation of the impulse response is critical. Indeed, by the Gauss divergence theorem, the integral of the normal derivative on the boundary [Eq. (3)] (which vanishes since the normal derivative does) must be equal to the volume integral over the domain.

The assumption of unbounded domain can not be maintained with a numerical approach. A radiation condition (LOWERY *et al.*, 2002) or a truncation of the domain is used to overcome the problem. As noted above, when truncating the domain, the impulsive response for an insulated volume conductor can not be obtained. However, it is still possible to solve the problem for the modified Green function:

$$\begin{cases} -\nabla \cdot \underline{\underline{\sigma}} \nabla G = \delta - 1/V \\ \frac{\partial G}{\partial n} = 0 \end{cases} \quad (13)$$

where  $\delta$  is the impulsive source and  $V$  is the volume of the domain  $\Omega$ .

When the modified Green function [from Eq. (13)] is substituted into the Green formula giving the potential in terms of  $G$ , of the source, and of the boundary data, the term  $1/V$  of the right hand side of Eq. (13) produces the volume integral in Eq. (14), which is a constant value:

:

$$\varphi(\vec{x}) = \int_{\partial\Omega} G(\vec{x}, \vec{x}') I(\vec{x}') d\vec{x}' + \int_{\Omega} \varphi(\vec{x}) d\vec{x} \quad (14)$$

Studying the impulsive response of the system may be useful not only when considering analytical solutions. Indeed, in particular conditions, the theory of transfer functions can be used to obtain the full solution of the problem of EMG simulation by simple convolutions, once the equivalent transfer function of the volume conductor is derived analytically or computed numerically (see section “Calculation of the surface detected potential”).

Under the hypothesis that the volume conductor is homogeneous in the direction of propagation and that the geometry is invariant along the same direction, the solution obtained for a specific source in a specific position contains also the information about the solution obtained with the source in other locations along the propagation path. The geometric invariance in the direction of the source propagation implies that there is a one parameter isometric map  $T_s$  conserving the angles (a conformal map), i.e., a family of rotations or translations, of the domain in itself, mapping each fiber point into another:

$$\begin{aligned} T_s \Omega &= \Omega \\ T_s \gamma(s_0) &= \gamma(s_0 + s) \end{aligned} \quad (15)$$

where  $\Omega$  is the domain in which the volume conductor is placed and  $\gamma$  is the curve defining the muscle fiber.

We define as space invariance in the direction of propagation of the source, the property of the volume conductor of being both homogeneous and geometrically invariant [following the definition (15)] along this direction. This definition produces a class of volume conductors for which the simulation of surface detected EMG potentials can be viewed as a linear filtering problem. In particular, for space-invariant volume conductors, the potential distributions generated by two impulsive sources located at different locations along the direction of propagation are translated

versions of each other, thus the response to a single source is sufficient to generate the potential as detected during the source propagation (Figure 3).

**Figure 3 about here**

### **2.3 Calculation of the surface detected potential**

The surface detected action potential generated by a single fiber can be computed from the description of the source and of the volume conductor. The computational approaches differ in the case of space and non-space invariant systems. Given the properties of the fibers belonging to a motor unit, the motor unit action potential is computed from the summation of the single fiber action potentials. Introducing the activation pattern of each motor unit, the surface EMG signal is obtained, as described in previous work (FARINA *et al.*, 2002). In the following we will describe the calculation of the single fiber action potential, referring to previous work for the generation of the interference surface EMG signal.

#### **2.3.1 Space-invariant volume conductors**

If the volume conductor is invariant in the direction of propagation of the intra-cellular action potential and if the source satisfies Eq. (15), the response of the system to a Delta current function provides the response to any source located along the direction of propagation. Indeed, in this case the potential distribution over the skin is shifted in space, without changes in shape, when the source is moved along the propagation path (Figure 3). The system can be fully characterized by a one-dimensional transfer function in the direction of propagation of the source (FARINA and MERLETTI, 2001a). Assuming that the transfer function  $H(k_1, k_2)$  (with  $k_1$  and  $k_2$  the spatial angular frequencies in the two coordinates in which the surface of the volume conductor is described) is applied to the source  $I(k_1)$  (with  $k_1$  corresponding to the direction of propagation of the source), the resulting potential distribution over the skin surface is given by:

$$\phi(k_1, k_2) = I(k_1)H(k_1, k_2) \quad (16)$$

Note that Eq. (16) can be applied due to the properties of linearity and space-invariance of the system in the direction of propagation. Indeed, under such hypotheses, the surface potential distribution over the skin plane can be obtained by a filtering operation. With calculations similar to those presented in (FARINA and MERLETTI, 2001a) and generalized for a generic spatial coordinate system, the potential detected along the direction of propagation of the source can be obtained by filtering the source with the following one-dimensional transfer function:

$$B(k_1) = \int H(k_1, k_2) e^{jk_2 x_{20}} dk_2 \quad (17)$$

where  $x_2$  indicates the coordinate orthogonal to the direction of the fibers, and  $x_{20}$  is the distance between the detection point and the direction of propagation of the source. In the transfer function  $H(k_1, k_2)$ , which represents the volume conductor, it is also possible to include the spatial transfer functions describing the electrode configuration (spatial filter) and the electrode size and shape [generalization of the concepts shown in (FARINA and MERLETTI, 2001a)].

Transfer function (17) can then be applied to the source, described by Eq. (1), for each instant of time and with  $k_1$  the spatial angular frequency corresponding to the curvilinear abscissa. In the Fourier domain this may be reduced to a single filtering operation in the temporal domain, which can be obtained by generalizing the concepts proposed in (FARINA and MERLETTI, 2001a; FARINA *et al.*, 2003a). This decreases significantly the computational time.

The above concepts are independent on the way in which the volume conductor transfer function is computed, thus can be applied to both analytical or numerical descriptions of the tissues, with the condition on the volume conductor to be space-invariant in the direction of source propagation. In this case, the computational time is reduced by the analytical description of the generation and extinction of the intra-cellular action potential [Eq. (1)], and of the detection system (FARINA and MERLETTI, 2001a). Examples of volume conductors to which such an approach can be applied are reported in Figure 1a,d,e,f.



### 2.3.2 Non space-invariant volume conductors

If the volume conductor is not space-invariant, the modelization of the source indicated in Eq. (1) can still be applied but the response to a Delta function can not be interpreted as a transfer function, as it was done in Eq. (16). Thus, it is necessary to calculate the solutions corresponding to impulsive sources placed at all the points along the fiber. In this case, since the simulated signal is sampled in the time domain, there will be a corresponding spatial sampling. This does not correspond to any loss of information if the sampling is performed according to the Nyquist theorem. Given the temporal bandwidth  $B_T$  of the EMG signal, the minimum sampling frequency in time domain is  $f_{samp} = 2B_T$ . The following relation, thus, holds for the sampling of the coordinate along the direction of propagation:

$$\Delta s = \frac{v}{f_{samp}} \quad (16)$$

where  $s$  is the curvilinear abscissa,  $\Delta s$  the sampling period in the space domain, and  $v$  the propagation velocity of the source.

## 3. RESULTS

The previous concepts were applied for the representative results which will be shown in the following. Figure 4 reports examples of the surface potential distributions as simulated over the skin surface for two volume conductors. The numerical approach applied is based on finite elements and was implemented by the software package FEMLAB (version 2.3b). The intra-cellular action potential was described by a current tripole (with parameters taken from MERLETTI *et al.*, 1999a; 1999b). The cases in Figure 4a relate to a volume conductor which is space invariant in the longitudinal direction, while the case in Figure 4b represent a more general volume conductor.

**Figure 4 about here**

Figure 5 reports an example of simulation of surface potential distributions as detected over the skin surface of four volume conductors. The first is a planar volume conductor, space-invariant in the direction of propagation of the source and homogeneous. The second case represents the analytical modelization of a bipinnate muscle, following the solution provided by MESIN and FARINA (2004). The volume conductor is not space-invariant and in-homogeneous. The effect of the second pinnation angle is evident from the potential distribution over the skin plane when compared to the case of parallel fibers. Note that a change in the conductivity tensor has a large effect on the potential distribution when considering the same geometry and location of the source. An emi-cylindrical volume conductor with bi-pinnate rectilinear fibers is considered in Figure 4c, applying the conductivity tensor of Eq. (8). The change in geometry of the volume conductor implies a variation in the potential distribution generated by a source at the same distance from the detection point when compared to the case of the planar bipinnate muscle. Finally, the case of a bipinnate muscle in an emi-cylindrical volume conductor and curvilinear fibers (Figure 2) is presented. The solution for this volume conductor (Figure 5d) has been obtained numerically with the conductivity tensor derived in Eq. (12). The fiber direction defines the conductivity in each point of the volume conductor. The resultant potential distribution is affected by the geometry and the conductivity tensor adopted.

**Figure 5 about here**

Figure 6 shows simulations of a cylindrical volume conductor with local in-homogeneities, simulated as spheres of different conductivities with respect to the fat layer in which they are located. The system is not space-invariant in the direction of propagation of the sources. Monopolar, single differential, and double differential filters were applied for signal recording. The potential distribution over the skin plane depends on the position of the source along the

propagation direction (non-space invariant system). As a consequence, the potentials detected along the direction of propagation have different shapes depending on the position of the detection system. Due to the shape changes, the delay between signals detected along the fiber direction is not uniquely defined. For example, the peak values of the detected potentials provide estimates of the propagation delay which depend on the location of the detection system. Moreover, different spatial filters determine different delays between signal peaks since the shape of the detected potentials change in different ways depending on the spatial filter applied.

The use of volume conductors that are not space-invariant is particularly interesting for analyzing the effect of non-ideal conditions on estimates of conduction velocity (FARINA & MERLETTI, 2004; MESIN *et al.*, 2004) or on the selectivity properties of the spatial filters. In particular, the description of tissue in-homogeneities may provide an interpretation to the large variability of conduction velocity estimates found experimentally in dependence of the location of the detection system over the muscle, of the spatial filter applied, and of the specific methods of estimation (FARINA *et al.*, 2004b; SCHULTE *et al.*, 2003). In addition, non-space invariant systems may be useful to interpret deviations from the theoretical predictions of spatial filter selectivity in specific experimental conditions. The use of these models may thus prove useful for addressing specific issues in surface EMG interpretation that can not be faced by simpler analytical models.

**Figure 6 about here**

#### **4. DISCUSSION & CONCLUSION**

Although it is of paramount importance to develop surface EMG analytical models, there are conditions in which an analytical analysis is not feasible. If complex descriptions of the volume conductor are required for addressing specific issues of surface EMG signal interpretation, a numerical method should be applied. In this study we discussed the classification of volume conductors and their properties in relation to the EMG simulation (such as the space-invariance

property in the direction of propagation of the sources). The aim was to present methods for reducing the computational time when applying a numerical approach. It was shown that for space-invariant systems, the simulation of the surface detected potential generated by any source traveling along the fiber (with generation and extinction at the end-plate and tendons) can be computed from a convolutional operation. This approach can be applied also to cases in which the volume conductor transfer function is obtained numerically. In these cases, it is sufficient to compute the impulsive response of the system to simulate surface potentials generated by intra-cellular action potentials originating at the end-plate, traveling along the fiber, and extinguishing at the tendon regions. However, the class of space-invariant volume conductors is limited and does not include important cases of geometries and conductivity tensors.

The calculation of the volume conductor transfer function by a numerical method poses the problems of the description of the geometry and of the determination of the conductivity tensor. Since the conductivity of the muscle tissue depends on the direction of the fibers, the description of the source is linked to that of the conductivity tensor. Description of the conductivity tensor may be a non trivial task, as shown representatively for the bipinnate muscle analyzed in this work. In the past, attention has been devoted to the description of the geometry while less efforts were focused on the determination of the conductivity tensor and its relation to the source propagation direction. The availability of numerical methods for describing complex geometries and conductivity tensors underlines the need of estimating the conductivity properties and geometrical features of the system under study, which may be a critical aspect for EMG simulation.

In conclusion, the present work provides two main results: 1) a method for surface EMG signal simulation for space-invariant systems and 2) the advanced application of numerical methods for the description of volume conductor properties which have not been included in previous works (e.g., volume conductors with curvilinear fibers).

## REFERENCES

- BLOK, J.H., STEGEMAN, D.F., and VAN OOSTEROM, A. (2002): 'Three-layer volume conductor model and software package for applications in surface electromyography', *Ann. Biomed. Eng.*, **30**, pp. 566-577
- CLARK, J. and PLONSEY, R. (1968): 'The extracellular potential field of the single active nerve fiber in a volume conductor', *Biophys. Journ.*, **8**, pp. 842-64
- DIMITROV, G.V. and DIMITROVA, N.A. (1980): 'Modelling of the extracellular potentials generated by curved fibres in a volume conductor', *Electromyogr. Clin. Neurophysiol.*, **20**, pp. 27-40
- DIMITROV, G.V. and DIMITROVA, N.A. (1998): 'Precise and fast calculation of the motor unit potentials detected by a point and rectangular plate electrode', *Medical Engineering & Physics*, **20**, pp. 374-381
- DIMITROV, G.V., DISSELHORST-KLUG, C., DIMITROVA, N.A., SCHULTE, E. and RAU G. (2003): 'Simulation analysis of the ability of different types of multi-electrodes to increase selectivity of detection and to reduce cross-talk', *J. Electromyogr. Kinesiol.*, **13**, pp. 125-38.
- DIMITROVA, N.A. (1974): 'Model of the extracellular potential field of a single striated muscle fiber', *Electromyogr. Clin. Neurophysiol.*, **14**, pp. 53-66
- DIMITROVA, N.A., DIMITROV, A.G., and DIMITROV, G.V. (1999a): 'Calculation of extracellular potentials produced by an inclined muscle fibre at a rectangular plate electrode', *Med. Eng. Phys.*, **21**, pp. 583-8.
- DIMITROVA, N.A., DIMITROV, G.V., and CHIKHMAN, V.N. (1999b): 'Effect of electrode dimensions on motor unit potentials', *Med. Eng. Phys.*, **21**, pp. 479-85
- DIMITROVA, N.A., DIMITROV, G.V., and DIMITROV, A.G. (2001): 'Calculation of spatially filtered signals produced by a motor unit comprising muscle fibres with non-uniform propagation', *Med. Biol. Eng. Comput.*, **39**, pp. 202-7.
- DIMITROVA N.A. and DIMITROV G.V. (2003): 'Interpretation of EMG changes with fatigue: facts, pitfalls, and fallacies', *J. Electromyogr. Kinesiol.*, **13**, pp. 13-36

- ERINGEN, A.C. (1967) 'Mechanics of continua', Wiley: New York
- ERINGEN, A.C. (1971) 'Continuum physics: vol. 1st, Mathematics', Academic Press: New York.
- EVANS, L.C. (1998): 'Partial differential equations', Graduate Studies in Mathematics 19, A.M.S.
- FARINA, D. and MERLETTI, R. (2001a): 'A novel approach for precise simulation of the EMG signal detected by surface electrodes', *IEEE Trans. Biomed. Eng.*, **48**, pp. 637-646
- FARINA, D. and MERLETTI, R. (2001b): 'Effect of electrode shape on spectral features of surface detected motor unit action potentials', *Acta Physiol. Pharmacol. Bulg.*, **26**, pp. 63-6.
- FARINA, D., FOSCI, M., and MERLETTI, R. (2002): 'Motor unit recruitment strategies investigated by surface EMG variables', *J. Appl. Physiol.*, **92**, pp. 235-47.
- FARINA, D., MESIN, L., MARTINA, S. and MERLETTI, R. (2003a): 'A surface EMG generation model with multi-layer cylindrical description of the volume conductor', *IEEE Trans. Biomed. Eng.*, **51**, pp. 415-26.
- FARINA, D., MESIN, L., MARTINA, S. and MERLETTI, R. (2004a): 'Comparison of spatial filter selectivity in surface myoelectric signal detection – Influence of the volume conductor model', *Med. Biol. Eng. Comput.*, **42**, pp. 114-20
- FARINA, D., ZAGARI, D., GAZZONI, M. and MERLETTI, R. (2004b): 'Reproducibility of muscle fiber conduction velocity estimates using multi-channel surface EMG techniques', *Muscle and Nerve*, **29**, pp. 282-91
- FARINA, D., and MERLETTI, R. (2004): 'Methods for muscle fiber conduction velocity estimate from surface EMG signals', *Med. Biol. Eng. Comput.*, in press
- GOOTZEN, T.H. (1990): 'Muscle fibre and motor unit action potentials. A biophysical basis for clinical electromyography', PhD thesis, University of Nijmegen
- GOOTZEN, T.H., STEGEMAN, D.F. and VAN OOSTEROM, A. (1991): 'Finite limb dimensions and finite muscle length in a model for the generation of electromyographic signals', *Electroenc. Clin. Neurophysiol.*, **81**, pp. 152-162

- GRIEP, P., GIELEN, F., BOON, K., HOOGSTRATEN, L., POOL, C. and WALLINGA DE JONGE, W. (1982): 'Calculation and registration of the same motor unit action potential', *Electroencephalogr. Clin. Neurophysiol.*, **53**, pp. 388-404
- GYDIKOV, A., GERILOVSKI, L., RADICHEVA, N. and TRAYANOVA, N. (1986): 'Influence of the muscle fiber end geometry on the extracellular potentials', *Biol. Cybern.*, **54**, pp. 1-8
- HELAL, J.N., and BOUISSOU, P. (1992): 'The spatial integration effect of surface electrode detecting myoelectric signal', *IEEE Trans. Biomed. Eng.*, **39**, pp. 1161-7.
- JOHANNSEN, G. (1986): 'Line source models for active fibers', *Biol. Cybern.*, **54**, pp. 151-8
- KLEINE, B.U., STEGEMAN, D.F., MUND, D. and ANDERS, C. (2001): 'Influence of motoneuron firing synchronization on SEMG characteristics in dependence of electrode position', *J. Appl. Physiol.*, **91**, pp. 1588-99
- KLEINPENNING, P., GOOTZEN, T., VAN OOSTEROM, A. and STEGEMAN, D.F. (1990): 'The equivalent source description representing the extinction of an action potential at a muscle fiber ending', *Math. Biosci.*, **101**, pp. 41-61
- LOWERY, M.M., STOYKOV, N.S., TAFLOVE, A. and KUIKEN, T.A. (2002): 'A multiple-layer finite-element model of the surface EMG signal', *IEEE Trans. Biomed. Eng.*, **49**, pp. 446-454
- MCGILL, K. and HUYNH, A. (1988): 'A model of the surface recorded motor unit action potential', *Proc. 10th Annu. Int. IEEE Conf. Eng. In Med. Biol.*, pp. 1697-1699
- MERLETTI, R., LO CONTE, L., AVIGNONE, E. and GUGLIELMINOTTI, P. (1999): 'Modelling of surface myoelectric signals – part I: model implementation', *IEEE Trans. Biomed. Eng.*, **46**, pp. 810-820
- MERLETTI, R., ROY, S.H., KUPA, E., ROATTA, S. and GRANATA, A. (1999): 'Modeling of surface myoelectric signals--Part II: Model-based signal interpretation', *IEEE Trans. Biomed. Eng.*, **46**, pp. 821-9
- MESIN, L. and FARINA, D. (2004): 'Simulation of surface EMG signals generated by muscle tissues with in-homogeneity due to fiber pinnation', *IEEE Trans. Biomed. Eng.*, in press

MESIN, L., FARINA, D., and MERLETTI, R. (2004): 'Effect of local in-homogeneities in the subcutaneous tissue on muscle fiber conduction velocity estimates assessed with a novel analytical surface EMG model', *Proc. of the 15th Congress of the International Society of Electrophysiology and Kinesiology*, Boston, 2004, in press

VAN OOSTEROM, A. (1998): 'Principles in inverse electrophysiological modeling', 6<sup>th</sup> Deliverable of the SENIAM project, pp. 37-44

PLONSEY, R. (1977): 'Action potential sources and their volume conductor fields', *IEEE Trans. on Biomed. Eng.*, **56**, pp. 601-611

REUCHER, H., RAU, G., and SILNY, J. (1987a): 'Spatial filtering of noninvasive multielectrode EMG: part I--Introduction to measuring technique and applications', *IEEE Trans. Biomed. Eng.*, **34**, pp. 98-105

REUCHER, H., RAU, G., and SILNY, J. (1987b): 'Spatial filtering of noninvasive multielectrode EMG: part II--Filter performance in theory and modelling', *IEEE Trans. Biomed. Eng.*, **34**, pp. 106-113

ROELEVELD, K., BLOK, J.H., STEGEMAN, D.F. and VAN OOSTEROM, A. (1997): 'Volume conduction models for surface EMG; confrontation with measurements', *J. Electromyograph. Kinesiol.*, **7**, pp. 221-232

SCHNEIDER, J., SILNY, J. and RAU, G. (1991): 'Influence of tissue inhomogeneities on noninvasive muscle fiber conduction velocity measurements investigated by physical and numerical modeling', *IEEE Trans. on Biomed. Eng.*, **38**, pp. 851-860

SCHULTE, E., FARINA, D., RAU, G., MERLETTI, R. and DISSELHORST-KLUG, C. (2003): 'Single motor unit analysis from spatially filtered surface EMG signals – Part II : conduction velocity estimation', *Med. Biol. Eng. Comput.*, **41**, pp. 338-45

STEGEMAN, D.F., BLOK, J.H., HERMENS, H.J. and ROELEVELD, K. (2000): 'Surface EMG models: properties and applications', *J. Electromyograph. Kinesiol.*, **10**, pp. 313-326

XIAO, S., MC GILL, K.C., HENTZ, V.R. (1995): 'Action potentials of curved nerves in finite limbs', *IEEE Transactions on Biomedical Engineering*, **42**, pp. 599-607



## FIGURE CAPTIONS

**Figure 1** Examples of volume conductors with different geometries and conductivity tensors. In some cases, both analytical and numerical solutions are available from the literature (see text for details), while in others only numerical methods can be used.

**Figure 2** A model of volume conductor with curvilinear fibers, following two orientations (bipinnate muscle). The conductivity tensor should be adapted point-by-point to the fiber orientation. In particular, at each point, the muscle has a conductivity tensor which describes larger conductivity in the local direction of the fibers and lower in the transverse directions.

**Figure 3** Schematic example of surface potentials generated by a point source which propagates along a direction defined in a generic coordinate system  $(x_1, x_2, x_3)$ . a) The source is located at positions 1 and 2, along the propagation direction in a generic volume conductor; the cases of a space-invariant and non space-invariant volume conductor are representatively shown. The surface potential detected at position 2 (schematic drawing) is equal in shape to that detected at location 1 in case of space-invariant system (c). For a non space-invariant volume conductor, the shape changes during propagation (d). The represented potential distributions are not related to signal simulations in a specific volume conductor but are schematic drawings of the space-invariance concept.

**Figure 4** Surface potentials generated by a current tripole (for the parameters of the tripole refer to MERLETTI *et al.*, 1999) at a fixed position in two volume conductors. a) Cylindrical model (space-invariant) comprising a bone and the muscle tissue. b) The same system with the muscle tissue increasing in thickness toward the center of the volume conductor. In the two cases, the surface potential was computed using a finite element method (implemented by the software package

FEMLAB, version 2.3b), and has been represented with contour plots. In the first case (a) an analytical solution is also available (FARINA *et al.*, 2003a). The conductivity tensor of the muscle tissue is described in the same way (anisotropic, homogeneous) for both volume conductors. The radius of the bone is 20 mm and the source is located 10 mm deep within the muscle in both cases. The conductivity of the muscle tissue is 0.5 S/m in the longitudinal direction and 0.1 S/m in the angular and radial directions, while the bone is isotropic with conductivity 0.02 S/m. The thickness of the muscle tissue in a) is 30 mm. In b) the muscle tissue is 5 mm thick at the boundaries of the volume conductor and 30 mm thick at the center. The thickness profile in  $z$  follows a cosine function.

**Figure 5** Comparison of simulated surface potentials for different models of a bi-pinnate muscle. a) Planar muscle with parallel fibers (analytical solution provided by FARINA and MERLETTI, 2001a) (top view); b) bi-pinnate planar muscle (analytical solution provided by MESIN & FARINA, 2004) (top view); c) emi-cylindrical bi-pinnate muscle, with rectilinear fibers (numerical solution with conductivity tensor as in Eq. (8)); d) emi-cylindrical bi-pinnate muscle, with curvilinear fibers (numerical solution with conductivity tensor as in Eq. (12)). The source is a current tripole (see MERLETTI *et al.*, 1999a, MERLETTI *et al.*, 1999b, for the parameters) located at 5 mm depth within the muscle ( $\sigma_l = 0.5$  S/m,  $\sigma_t = 0.1$  S/m), 3 mm distant from the pinnation interface along the direction of the fiber. The pinnation angle is  $15^\circ$ .

**Figure 6** The case of a cylindrical model (a) comprising a bone (radius 20 mm, homogeneous, isotropic, conductivity 0.02 S/m), the muscle tissue (thickness 30 mm, homogeneous, anisotropic, longitudinal conductivity 0.5 S/m, radial and angular conductivity 0.1 S/m), and the fat layer (thickness 5 mm, homogeneous, isotropic, conductivity 0.05 S/m), with spherical in-homogeneities (radius 3 mm, homogeneous, isotropic, conductivity 0.5 S/m) within the fat layer is numerically analysed. The source is a current tripole (for the parameters of the tripole refer to MERLETTI *et al.*,

1999). The simulated EMG signals recorded with a four electrode linear electrode array (interelectrode distance 5 mm) are shown. The source travels with a conduction velocity of 4 m/s. The sampling frequency is  $f_{samp} = 1$  kHz. The correspondent spatial resolution is  $\Delta z = 1/(2f_{max}) = v/f_{samp} = 4$  mm, thus the solution was computed for the source shifting along the muscle fiber at steps of 4 mm. Each time sample of the simulated potentials corresponds to a location of the source within the volume conductor. Once the potential distributions have been computed for each position of the source, they can be used to obtain the surface EMG signals as functions of time at specific detection points. Monopolar (b), single differential (c), and double differential (d) signals are shown. Note that the presence of the in-homogeneities causes the delays between signals detected by adjacent electrodes to be different, depending on the position of the electrodes and on the spatial filter. The spherical in-homogeneities are represented by 3 spheres at a mean depth of 2.5 mm within the fat layer. M1, M2, M3, M4 indicate the four monopolar recordings, SD1, SD2, SD3 represent the three single differential recordings, and DD1, DD2 the two double differential signals.

Fig 1

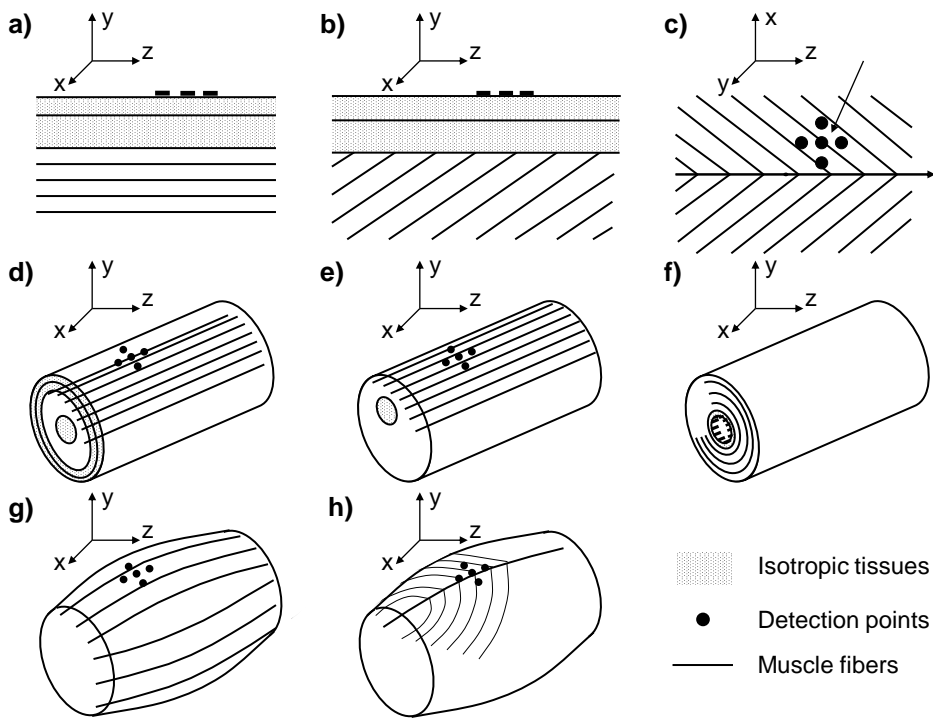


Fig 2

**Bi-pinnate muscle with curvilinear muscle fibers**

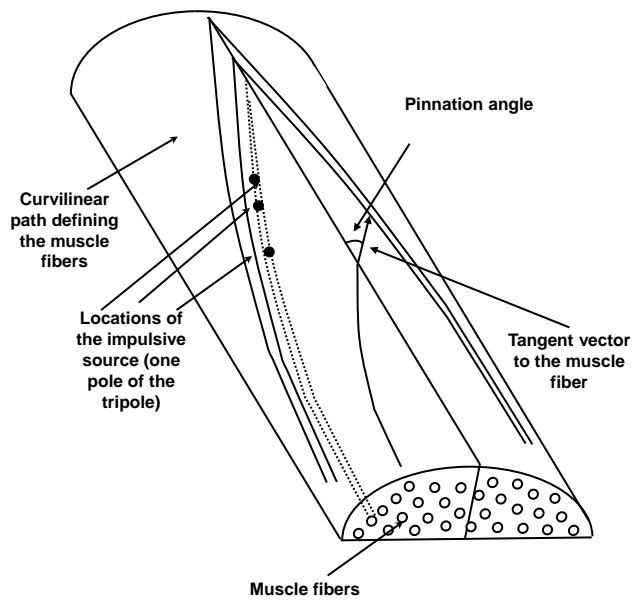


Fig 3

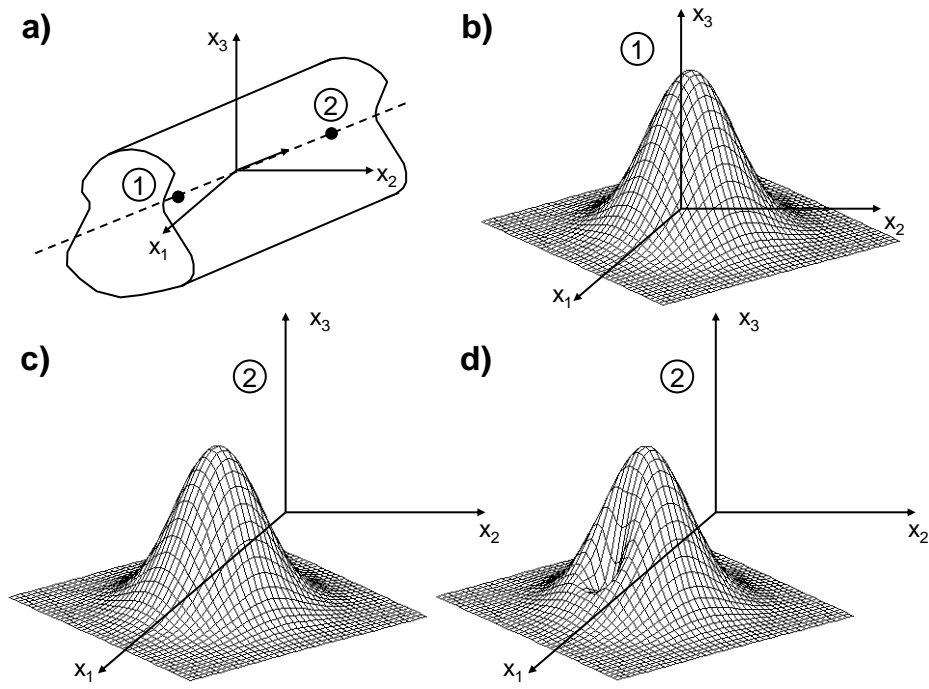


Fig 4

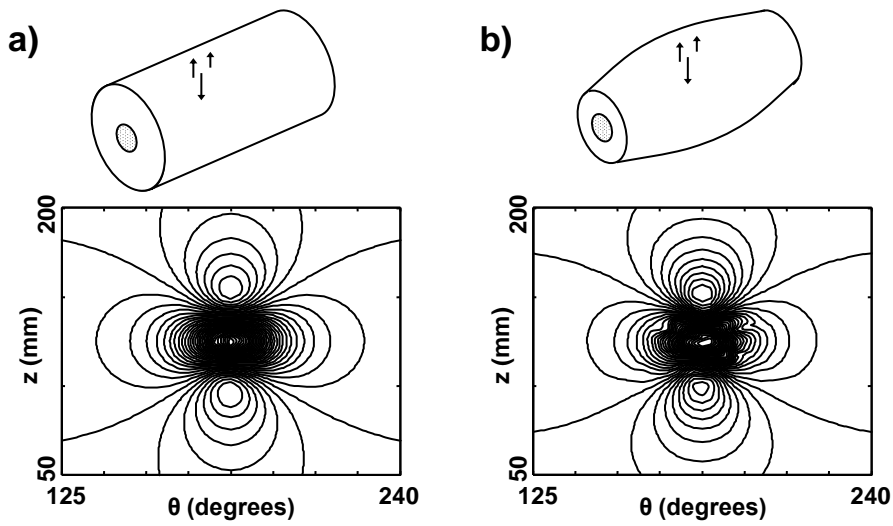


Fig 5

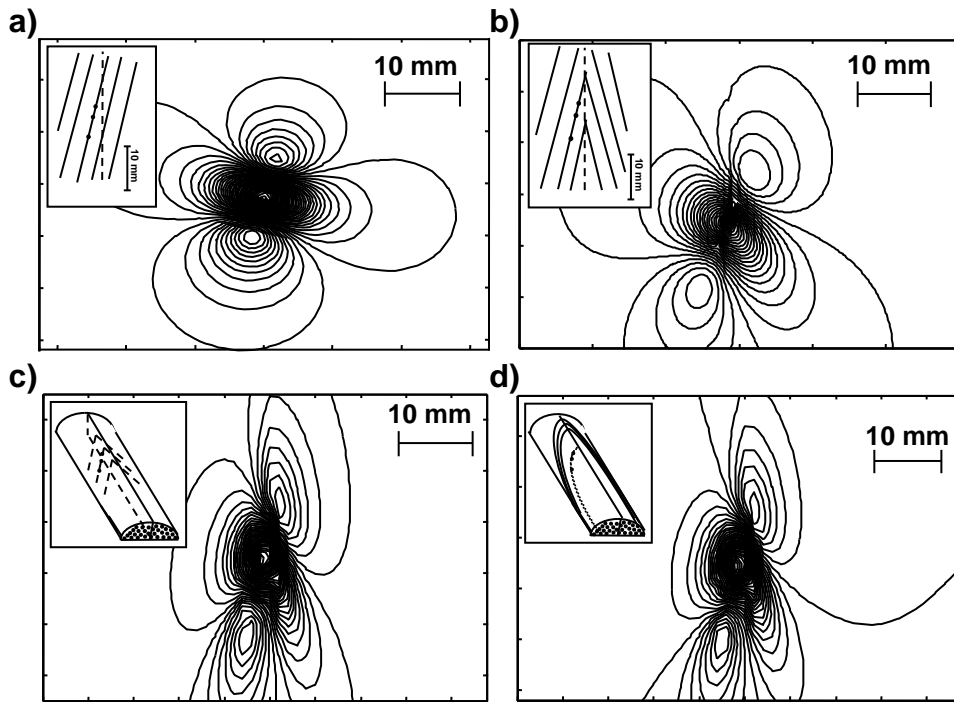


Fig 6

